Physiol Genomics 30: 134–145, 2007.
First published March 20, 2007; doi:10.1152/physiolgenomics.00011.2007.

MyD88-dependent changes in the pulmonary transcriptome after infection with *Chlamydia pneumoniae*

Nuria Rodríguez,* Jörg Mages,* Harald Dietrich, Nina Wantia, Hermann Wagner, Roland Lang,* and Thomas Miethke*

Institute of Medical Microbiology, Immunology and Hygiene, Technical University of Munich, Munich, Germany

Submitted 10 January 2007; accepted in final form 17 March 2007

Rodríguez N, Mages J, Dietrich H, Wantia N, Wagner H, Lang R, Miethke T. MyD88-dependent changes in the pulmonary transcriptome after infection with *Chlamydia pneumoniae*. *Physiol Genomics* 30: 134–145, 2007. First published March 20, 2007; doi:10.1152/physiolgenomics.00011.2007.—*Chlamydia pneumoniae*, an intracellular bacterium, causes pneumonia in humans and mice. Toll-like receptors and the key adaptor molecule myeloid differentiation factor-88 (MyD88) play a critical role in inducing immunity against this microorganism and are crucial for survival. To explore the influence of MyD88 on induction of immune responses in vivo on a genome-wide level, wildtype (WT) or MyD88$^{-/-}$ mice were infected with *C. pneumoniae* on anesthesia, and the pulmonary transcriptome was analyzed 3 days later by microarrays. We found that the infection caused pulmonary cellular infiltration in WT but not MyD88$^{-/-}$ mice. Furthermore, it induced the transcription of 360 genes and repressed 18 genes in WT mice. Of these, 221 genes were not or weakly induced in lungs of MyD88$^{-/-}$ mice. This cluster contains primarily genes encoding for chemokines and cytokines like MIP-1α, MIP-2, MIP-1γ, MCP-1, TNF, and KC and other immune effector molecules like immunoresponsive gene-1 and TLR2. Arginase was highly induced after *C. pneumoniae* infection and was MyD88 dependent. Genes induced by interferons were abundant in a cluster of 102 genes that were only partially MyD88 dependent. Also, *lcn2* (lipocalin-2) and *timp1* were represented within this cluster. Interestingly, a set of 37 genes including *sprr1a* was induced more strongly in MyD88$^{-/-}$ mice, and most of them are involved in the regulation of cellular replication. In summary, ex vivo analysis of the pulmonary transcriptome on infection with *C. pneumoniae* demonstrated a major impact of MyD88 on inflammatory responses but not on interferon-type responses and identified MyD88-independent genes involved in cellular replication.

microarray; inflammation; Toll-like receptor; myeloid differentiation factor-88

RESPIRATORY INFECTION WITH *Chlamydia pneumoniae*, an obligate intracellular gram-negative bacterium, causes pneumonia and bronchitis in humans (3, 9, 33, 66, 67) and also in mice (68). The normal route of entry for this bacterium is the oral and nasal mucosa (9, 53). Infection with *C. pneumoniae* has been related to asthma and chronic obstructive pulmonary disease (7, 29) and also to nonrespiratory diseases like atherosclerosis (2, 22, 26, 34). It is widely distributed in the population, and up to 50% of the people of the developed world are seropositive by the age of 20 years (16, 21). *C. pneumoniae* can infect a wide range of different cell types, like lung epithelium, alveolar macrophages, circulating monocytes, arterial smooth muscle cells, and vascular endothelium (20, 25, 54). Recently, it was demonstrated that this microorganism is able to infect polymorphonuclear neutrophils (PMN) and live within them (48, 64). After 2–3 days of the infection, infected pulmonary areas are characterized by a cellular infiltrate consisting mainly of PMN (67). After uptake, *Chlamydia* grows within an intracellular vacuole called inclusion. The chlamydial developmental cycle involves a metabolically inactive, nonreplicative but infective elementary body (EB) that differentiates into a metabolically active reticular body (RB) after entry into the target cell.

Toll-like receptors (TLRs) are the main activators of the innate immune response when they recognize conserved pathogen-associated molecular patterns (PAMPs) (61). Eleven members have already been reported (6, 14, 23, 47, 62, 69), and immune cells display a differential expression pattern of TLRs (44). Myeloid differentiation factor-88 (MyD88) is a key adaptor molecule in the TLR signaling pathway (60). This molecule interacts via the Toll/interleukin-1 receptor (TIR) domain with all TLRs, except TLR3, and IL-1 receptor family members. In mice deficient for MyD88, an impaired production of proinflammatory cytokines after infection with a microorganism is frequently observed (5, 32). The absence of this adaptor molecule correlates with increased host lethality in different models (1, 52) even if an adaptive immune response was produced (19). In other models like choriomeningitis virus infection, MyD88 is critical for inducing an adaptive immune response (70). In certain instances, absence of MyD88 was even beneficial to the host (58, 65).

We recently demonstrated the importance of MyD88 in the innate immune response induced by *C. pneumoniae* infection. In the absence of MyD88, mice were not able to recruit PMN into the lungs 3 days postinfection, and the secretion of cyto- and chemokines was abolished with the exception of IL-12p40 (48). In contrast to wildtype (WT) mice, MyD88-deficient mice succumbed to the infection (48, 49). In this report we show, through the use of DNA microarray technology, that MyD88 determines transcriptional activation programs in lungs of mice infected with *C. pneumoniae*. While MyD88 controlled the expression of the majority of genes involved in the immune response against this microorganism in the early stage of pulmonary infection, a subgroup of IFN-induced genes was partially dependent on MyD88, and a cluster of genes associated with cell proliferation was even more strongly induced in the absence of MyD88.

* N. Rodríguez, J. Mages, R. Lang, and T. Miethke contributed equally to this study.

Article published online before print. See web site for date of publication (http://physiolgenomics.physiology.org).

Address for reprint requests and other correspondence: T. Miethke, Institute of Medical Microbiology, Immunology and Hygiene, Technical Univ. of Munich, Trogerstr. 30, 81675 Munich, Germany (e-mail: Thomas.Miethke@lrz.tum.de).

EXPERIMENTAL PROCEDURES

Mice. C57BL/6 mice were purchased from Harlan Winkelmann (Borchen, Germany). Breeding pairs of MyD88$^{-/-}$ mice were kindly provided by Dr. S. Akira (Osaka University, Osaka, Japan) and were backcrossed eight times to C57BL/6 mice and bred in the animal facility at the Institute of Medical Microbiology, Immunology and Hygiene. All animal experiments were done with the permission of local authorities (Oberbayern, Munich, Germany; file no. 211-2531-25/11).

Reagents and monoclonal antibodies. The reagent α-isonitrosopropiophenone (I-3502) and the proteinase inhibitor PMSF (P-7626) were provided by Sigma. The other proteinase inhibitors, leupeptine (1017-101) and aprotinin (236624), were purchased from Roche (Mannheim, Germany).

Multiplication and purification of C. pneumoniae. C. pneumoniae CM-1 (VR-1360; American Type Culture Collection, Manassas, VA) were multiplied according to Maass et al. (40). *Chlamydial* elementary bodies were centrifuged (2,000 *g*, 35 min, 35°C) on confluent monolayers of HEp2 cells in the presence of cycloheximide (1 μg/ml) and 0% FCS. After 72 h of culture, the harvested cells were disrupted with glass beads, and chlamydial elementary bodies were purified in a sucrose urografin gradient (bottom layer, 50% wt/vol sucrose solution; top layer, 30% vol/vol urografin in 30 mM Tris·HCl buffer, pH 7.4) at 9,000 *g* and 4°C for 60 min. After one wash step with 0.2 μm-filtered PBS (pH 7.4), purified elementary bodies were stored in SPG buffer (0.22 M sucrose, 8.6 mM Na_2HPO_4, 3.8 mM KH_2PO_4, 5 mM glutamic acid, 0.2-μm filtered, pH 7.4) at −80°C until use. To quantify the number of elementary bodies, HEp2 cells were infected and stained with the chlamydia-specific Ab (ACI-FITC; Progen Biotechnik, Heidelberg, Germany). The number of inclusion-forming units (IFUs) was counted as determined by fluorescence microscopy (Carl Zeiss Jena, Göttingen, Germany) 48 h after infection. For control, noninfected HEp2 cells were treated in the same way. Contamination with mycoplasma was excluded regularly by *Mycoplasma*-PCR using specific primers (MWG Biotech, Martinsried, Germany).

Infection protocol. Mice were anesthetized with an intraperitoneal injection of Ketamin (2 mg/mouse). Subsequently, mice were infected intranasally with 2.5×10^6 IFUs of *C. pneumoniae* in 30 μl of PBS. Three independent infection experiments were performed.

RNA isolation from lungs of mice. Mice were killed by CO_2 inhalation 3 days postinfection with *C. pneumoniae*. The lungs were flushed with 10 ml of PBS applied through the right atrium of the heart to remove blood. Immediately thereafter, lungs were transferred to precooled tubes placed in ethanol/dry ice bath, and, after homogenization, RNA was isolated using Tri-Reagent (T9424, Sigma) as described by the manufacturer. Degradation of the RNA was excluded by electrophoresis under RNase-free conditions, and the amount was quantified by spectrophotometry using Nanodrop ND-1000 V3.1.0 (Nanodrop Technologies).

Affymetrix gene chip and data analysis. Microarray analysis was performed in biological triplicates with RNA from individual mice derived from three independent infection experiments. Starting with 10 μg of total RNA, samples were labeled and hybridized to the murine expression arrays MOE-430A (Affymetrix, Santa Clara, CA) according to the manufacturer's protocol. Microarrays were scanned and initially analyzed for general assay quality using Affymetrix Microarray Suite v5.0 software [average background <115, scaling factors ranging between 0.19 and 0.54, and a mean percentage of present genes of 58% (±3.6)]. CEL files were subsequently imported into the program RMAExpress (v0.2 release) (4) for global normalization and generation of expression values. Significance analysis was performed with the significance analysis of microarrays (SAM) algorithm (v1.15) (63). To detect the genes that were significantly induced or repressed on *C. pneumoniae* infection in lungs of WT or MyD88$^{-/-}$ mice, a multiclass analysis was performed. With a median false discovery rate of 4.7%, a set of 1,053 probe sets was significantly regulated. Further filtering included a minimum fold change criterion between all four experimental conditions of ±2 (431 probe sets) and a maximum (all mean expression values) minus minimum (all mean expression values) filter of >100. The resulting 378 probe sets were considered to be differentially expressed in this setup.

The infection experiment of the ANA-1 macrophages was done in duplicate. Samples were hybridized to Affymetrix murine MG-U74AV2 arrays, and expression values were extracted as described above. For significance analysis we used R (language and environment for statistical computing) and LimmaGUI (linear package for microarray data) with a significance level of $P < 0.05$.

Further data preparation (e.g., gene-wise normalization) was done with the Spotfire DecisionSite v7 software (Spotfire) or R 2.0.1 (**http://www.r-project.org/index.html**). Hierarchical clustering was performed using the program Genesis (release 1.1.3) (57), and analysis of overrepresented genes within one biological category was done by the program Genomatix Bibliosphere (Genomatix, Munich, Germany).

Normalized expression values and CEL files were deposited in the Gene Expression Omnibus database (**http://www.ncbi.nlm.nih.gov/geo/**) as series GSE6688 (lung data) and GSE6690 (ANA-1 macrophages).

Detection of chemokines and cytokines. Levels of the chemokines keratinocyte-derived chemokine (KC), monocyte chemoattractant protein-1 (MCP-1), macrophage inflammatory protein-1α (MIP-1α), MIP-1γ, and MIP-2 as well as the cytokine tumor necrosis factor-α (TNFα) were determined in lungs of mice by commercially available ELISAs (duo set for KC, MIP-2, TNFα, MIP-1α, and MIP-1γ, R&D Systems, Wiesbaden-Nordenstadt, Germany; OptEIA set for MCP-1, Becton Dickinson, San Diego, CA). The assays were performed as recommended by the manufacturer. Lungs were isolated from mice and minced to homogeneity in 500 μl of PBS with an Ultra-Turrax T25 device (IKA Labortechnik, Jane&Kunkel). After centrifugation (2,000 *g*, 5 min), the supernatant was analyzed for its cyto- or chemokine content in duplicates.

Northern blot analysis of mRNA expression. For Northern analysis, 10 μg of total RNA prepared from the lungs of infected or control mice were separated on 1% formaldehyde-agarose gels and blotted onto Hybond N membranes (Amersham, Piscataway, NJ). Probes were prepared from plasmids obtained from Deutsches Ressourcenzentrum für Genomforschung (RZPD) (Heidelberg, Germany) containing full-length cDNAs for *tlr2* (clone IRAVp968E0244D) and *sprr1a* (IRAVp968F0841D) by digestion with the appropriate restriction enzymes and gel purification. Probes were labeled with ^{32}P-αdCTP using a random-primed labeling kit (Stratagene), purified, and hybridized to the membranes at 65°C overnight. After sequential washes in 2× and 0.2× SSC, membranes were exposed and analyzed on a PhosphoImager (Molecular Dynamics).

Real-time RT-PCR detection of mRNA. cDNA was prepared from RNA using Moloney murine leukemia virus (MMLV) RT according to a standard protocol. All real-time RT-PCRs were performed with the ABI SDS 7700 (Applied Biosystems). β-Actin or hypoxanthine guanine phosphoribosyl transferase (HPRT) was used as a reference gene. Primer sequences were 5′-GCCTCAAGGACGACAACATCAT-3′ (forward) and 5′-GGCTCTCTGGCAACAGGAAAG-3′ (reverse) for *lcn2*, 5′-AAAATTCGAGTGACAAGCCTGTAGC-3′ (forward) and 5′-GTGGGTGAGGAGCACGTAG-3′ (reverse) for *tnf*, 5′-CTTGACAAAGTGCCGC-3′ (forward) and 5′-CTTCGGGGGAGTAGTTT-3′ (reverse) for *irg1*, 5′-GCAAAGAGCTTTCT-CAAAGACC-3′ (forward) and 5′-AGGGATAGATAAACAGGGAAACACT-3′ (reverse) for *timp1*, 5′-AACTGCATCTGCCCTAAG-3′ (forward) and 5′-AAGGCATCACAGTCCGA-3′ (reverse) for *mcp1*, 5′-GCTGTCCCTCAACGGAA-3′ (forward) and 5′-ACATCTGGGCAA-TGGAAT-3′ (reverse) for *mip2*, 5′-ACCCACACTGTGCCCATCTAC-3′ (forward) and 5′-AGCCAAGTCCAGACGCAGG-3′ (reverse) for *actb*, and 5′-TCCTCCTCAGACCGCTTTT-3′ (forward) and 5′-CCTGGTTCATCATCGCTAATC-3′ (reverse) for *hprt1*. PCR conditions were as follows: 10 min, 95°C; 15 s, 95°C; and 60 s, 60°C for 40

cycles. The amount of each gene in each sample was relatively quantified using threshold cycle (C_T) values, applying the ΔΔCT method as recommended by Applied Biosystems.

Isolation of pulmonary cells. To isolate pulmonary cells, mice were killed by CO_2 inhalation 3 days after infection with *C. pneumoniae*. Lungs were flushed with PBS to remove blood as described above. Thereafter, the organ was cut into small pieces in a 60-μm plate and digested for 10 min with collagenase VIII (400 U/100 μl, RT, C-2139; Sigma, Taufkirchen, Germany) and subsequently for another 30 min (400 U collagenase/100 μl in 2 ml of RPMI, 0% FCS, 37°C). The digested material was filtered through a cell strainer of 100-μm pore size (Becton Dickinson Labware Europe, Le Pont De Claix, France) to remove debris.

Determination of arginase activity in lungs. Lungs were isolated from mice and minced to homogeneity in 0.5 ml of Tris·HCl, pH 7.5, containing protease inhibitors. After addition of 0.5 ml of 0.1% Triton X-100, the tubes were shaken for 10 min at 25°C and centrifuged at 13,000 rpm for 2 min. Arginase activity was determined as previously described (8). Briefly, 5 μl of 100 mM $MnCl_2$ were added to activate the enzyme to 50 μg of total protein, which was determined using bicinchoninic acid assay (BCA protein assay kit; Pierce, Rockford, IL). Arginine hydrolysis was carried out by incubating 100 μl of the activated lysate with 100 μl of 0.5 M arginine, pH 9.7, at 37°C for 1 h. The reaction was stopped with 400 μl of an acid mixture (H_2SO_4, H_3PO_4, and H_2O; 1:3:7 vol/vol/vol). The urea was measured at 540 nm after addition of 40 μl of 3% α-isonitrosopropiophenone (dis-

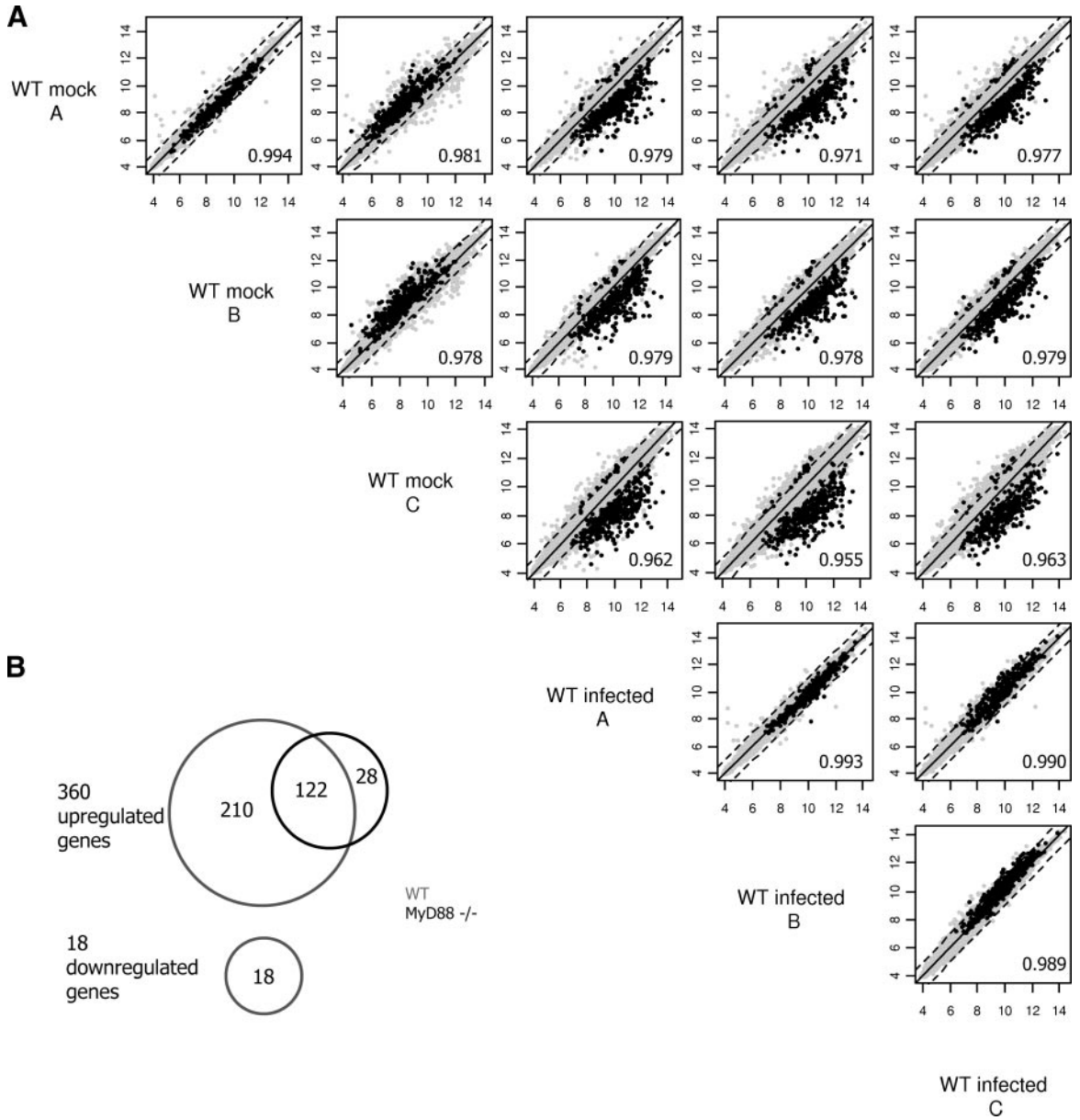

Fig. 1. *A*: scatter plot matrix. The normalized unfiltered expression values of all 6 wildtype (WT) arrays are plotted against each other to check for overall variation. The 3 independent experimental data sets are designated as *A*, *B*, and *C*. Each plot is composed of data of 2 arrays (*x* vs. *y*). The *top right* scatter plot, for example, shows the expression values of WT *mock A* (*y*-axis) vs. WT *infected C* (*x*-axis). Corresponding correlation coefficients (Pearson correlation) are shown in each scatter plot. Black dots represent transcripts that were significantly regulated in lungs after infection; grey ones show no significant change. Dashed lines represent a 2-fold change between the arrays. *B:* Venn diagrams for the 378 significantly regulated genes. MyD88, myeloid differentiation factor-88; gray circles, regulated >2-fold in WT mice on infection; black circle, regulated >2-fold in MyD88$^{-/-}$ mice. The overlap represents genes that are passing the 2-fold criterion in WT and MyD88$^{-/-}$ mice. No significantly downregulated genes could be observed in lungs of MyD88$^{-/-}$ mice.

solved in 100% ethanol) and incubation at 96°C for 1 h. One unit of arginase activity is the amount of enzyme that catalyzes the formation of 1 μmol urea/min.

Infection of the murine macrophage cell line ANA-1 with C. pneumoniae. ANA-1 cells growing in RPMI medium supplemented with 10% FCS were infected with *C. pneumoniae* with a multiplicity of infection (MOI) of 10 in the absence of FCS at the time of infection. After 8 h of incubation at 37°C, the cells were collected and centrifuged at 1,200 rpm ×5 min. Total RNA was isolated and hybridized in the microarray chip as described above.

Statistics. Comparison of two equally treated groups was analyzed by Mann-Whitney rank sum test or *t*-test if data was normally distributed. Statistical analysis was performed with SigmaStat (SPSS).

RESULTS AND DISCUSSION

Whole lung expression profiling identifies a large number of genes regulated after C. pneumoniae infection. Since we measured the RNA expression values from lungs of individual mice after infection with *C. pneumoniae* in three

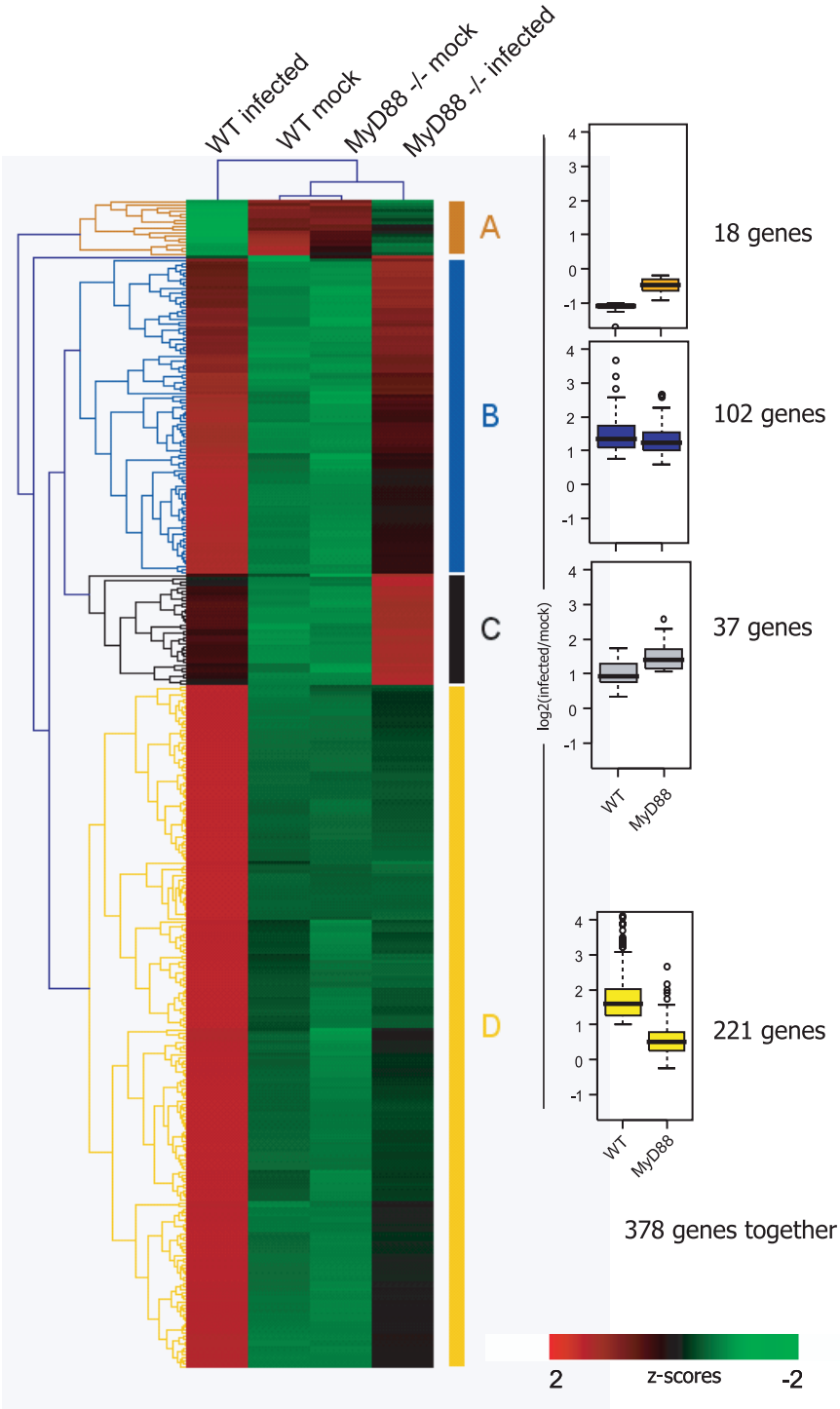

Fig. 2. Hierarchical cluster analysis of the 378 significantly regulated genes. Average expression values were gene-wise normalized using z-scores. Distinct clusters were labeled *A–D*. For each of the 4 clusters, a boxplot is shown, summarizing the $\log_2$ ratios of all genes in the particular cluster for WT or MyD88$^{-/-}$ samples on infection. The no. of genes for *clusters A–D* is shown at *right*.

Table 1. *Selected expression values and fold changes sorted by cluster membership*

Probe Set	Gene Title	Gene Symbol	WT Fold Change	MyD88$^{-/-}$ Fold Change	Cluster
1423062_at	insulin-like growth factor binding protein 3	Igfbp3	−3.2	−1.9	*A*
1426464_at	nuclear receptor subfamily 1, group D, member 1	Nrld1	−2.2	−1.5	*A*
1452114_s_at	insulin-like growth factor binding protein 5	Igfbp5	−2.1	−1.2	*A*
1423136_at	fibroblast growth factor 1	Fgf1	−2.1	−1.2	*A*
1460227_at	tissue inhibitor of metalloproteinase 1	Timp1	12.7	6.4	*B*
1431591_s_at	interferon, alpha-inducible protein	G1p2	9.1	6.2	*B*
1450783_at	interferon-induced protein with tetratricopeptide repeats 1	Ifit1	7.1	5.9	*B*
1417244_a_at	interferon regulatory factor 7	Irf7	6.0	4.3	*B*
1419042_at	interferon-inducible GTPase	Iigp-pending	5.5	3.0	*B*
1453196_a_at	2′-5′ oligoadenylate synthetase-like 2	Oasl2	5.4	4.3	*B*
1416342_at	tenascin C	Tnc	5.4	3.1	*B*
1449025_at	interferon-induced protein with tetratricopeptide repeats 3	Ifit3	5.3	4.6	*B*
1448123_s_at	transforming growth factor, beta induced	Tgfbi	5.0	3.4	*B*
1417141_at	interferon gamma induced GTPase	Igtp	4.0	2.5	*B*
1427747_a_at	lipocalin 2	Lcn2	3.8	3.0	*B*
1418825_at	interferon inducible protein 1	Ifi1	3.3	2.2	*B*
1427256_at	chondroitin sulfate proteoglycan 2	Cspg2	3.3	2.1	*B*
1450652_at	cathepsin K	Ctsk	3.1	2.1	*B*
1417793_at	interferon-g induced GTPase	Gtpi-pending	3.0	2.2	*B*
1419569_a_at	interferon-stimulated protein	Isg20	2.5	2.0	*B*
1417869_s_at	cathepsin Z	Ctsz	2.2	1.7	*B*
1448591_at	cathepsin S	Ctss	2.0	1.7	*B*
1454694_a_at	topoisomerase (DNA) II alpha	Top2a	3.1	4.3	*C*
1448314_at	cell division cycle 2 homolog A (S. pombe)	Cdc2a	2.7	3.9	*C*
1416664_at	cell division cycle 20 homolog	Cdc20	2.6	3.1	*C*
1416698_a_at	CDC28 protein kinase 1	Cks1	2.6	4.3	*C*
1417910_at	cyclin A2	Ccna2	2.4	2.8	*C*
1449133_at	small proline-rich protein 1A	Sprr1a	2.1	4.2	*C*
1448205_at	cyclin B1	Ccnb1	2.0	2.6	*C*
1450920_at	cyclin B2	Ccnb2	1.9	2.8	*C*
1452040_a_at	cell division cycle associated 3	Cdca3	1.6	2.3	*C*
1418930_at	chemokine (C-X-C motif) ligand 10	Cxcl10	27.6	6.3	*D*
1427381_at	immunoresponsive gene 1	Irg1	20.1	1.1	*D*
1419561_at	chemokine (C-C motif) ligand 3	Ccl3	17.2	1.1	*D*
1450826_a_at	serum amyloid A 3	Saa3	16.7	2.6	*D*
1449984_at	chemokine (C-X-C motif) ligand 2	Cxcl2	14.5	−1.1	*D*
1419549_at	arginase 1, liver	Arg1	13.0	1.5	*D*
1420380_at	chemokine (C-C motif) ligand 2	Ccl2	10.2	1.3	*D*
1418652_at	chemokine (C-X-C motif) ligand 9	Cxcl9	9.4	2.0	*D*
1419282_at	chemokine (C-C motif) ligand 12	Cc112	9.3	1.9	*D*
1421578_at	chemokine (C-C motif) ligand 4	Ccl4	6.3	−1.1	*D*
1449399_a_at	interleukin 1 beta	Il1b	5.6	1.2	*D*
1421228_at	chemokine (C-C motif) ligand 7	Ccl7	5.4	1.4	*D*
1417851_at	chemokine (C-X-C motif) ligand 13	Cxcl13	3.8	1.7	*D*
1417936_at	chemokine (C-C motif) ligand 9	Ccl9	3.5	2.3	*D*
1419209_at	chemokine (C-X-C motif) ligand 1	Cxcl1	3.4	1.0	*D*
1449049_at	toll-like receptor 1	Tlr1	3.2	1.2	*D*
1419132_at	toll-like receptor 2	Tlr2	3.2	1.6	*D*
1424727_at	chemokine (C-C motif) receptor 5	Ccr5	3.1	1.3	*D*
1451767_at	neutrophil cytosolic factor 1	Ncf1	3.1	1.3	*D*
1427736_a_at	chemokine (C-C motif) receptor-like 2	Ccrl2	2.6	−1.1	*D*
1419607_at	tumor necrosis factor	Tnf	2.4	1.0	*D*
1448859_at	chemokine (C-X-C motif) ligand 13	Cxcl13	2.3	−1.2	*D*
1418806_at	colony stimulating factor 3 receptor	Csf3r	2.3	1.0	*D*
1449195_s_at	chemokine (C-X-C motif) ligand 16	Cxcl16	2.3	1.9	*D*
1418465_at	neutrophil cytosolic factor 4	Ncf4	2.2	1.6	*D*
1448561_at	neutrophil cytosolic factor 2	Ncf2	2.1	1.4	*D*

Different expression patterns of genes (*clusters A–D*) on infection with *Chlamydia pneumoniae.* The average absolute expression value is shown for 4 different conditions. Fold change was calculated as a signed ratio of the average values from *C. pneumoniae* vs. mock-infected lungs of wildtype (WT) and MyD88$^{-/-}$ mice, respectively. "Cluster" refers to the cluster classification of Fig. 2.

independent experiments, we first asked for the overall reproducibility of the system. In Fig. 1 *A* the unfiltered normalized expression values (over 22,000 data points per comparison, gray dots) of all six mock and infected WT samples were plotted against each other. In general, we observed a high degree of concordance between replicates with low general aberration to each other. For example, for the three infected WT replicates, the correlation coefficient ranged between 0.989 and 0.993. In contrast, correlation coefficients between experimental conditions were much lower (ranging from 0.955 to 0.979), indicating the stronger effect of experimental conditions relative to variation between replicate samples. The same observation was made for the MyD88$^{-/-}$ microarrays (data not shown for reasons of clarity). Our stringent analysis for differentially expressed genes combined a statistical method (multiclass SAM) with filter criteria for absolute and fold changes in expression. Across all experimental conditions, we found 378 regulated genes. These are depicted as black dots in Fig. 1*A*, already visually indicating that most were expressed at higher levels at *day 3* after *Chlamydia* infection. Indeed, of the 378 regulated genes, 360 were upregulated on infection. In Fig. 1*B* the distribution of the significantly changed genes with respect to the MyD88 genotype is shown. A shared group of 122 genes were upregulated in WT and MyD88$^{-/-}$ mice after infection with *C. pneumoniae*; 210 genes passed the twofold change criterion only in the WT, not in MyD88$^{-/-}$, mice on infection, while only 28 genes were induced more than twofold exclusively in MyD88-deficient mice. Interestingly, only WT mice showed a greater than twofold reduction of RNA transcripts in this infection model (18 genes). Finally, under basal conditions, there were only very minor differences in gene expression between WT and MyD88$^{-/-}$ lungs (2 probe sets passing statistical and filter criteria).

MyD88 influences the majority of induced genes in lungs after infection with C. pneumoniae. We have reported previously that MyD88 controlled several cyto- and chemokine responses on infection with *C. pneumoniae* (48). The influence of MyD88 on global gene transcription in vivo on infection with this microorganism is demonstrated in Fig. 2, showing a hierarchical cluster analysis of average values of data from three independent experiments. In the cluster, only the genes that were significantly up- or downregulated in the three experiments are represented, resulting in a total of 378 genes as described above. The column dendrogram shows the high similarity between mock-infected WT and MyD88$^{-/-}$ lungs and the overall stronger effect of infection on WT than on MyD88$^{-/-}$ mice.

We have grouped genes according to similar expression patterns, and four main clusters were distinguished (Fig. 2). Since the hierarchical cluster was obtained using z-score normalized expression data, for each of the four clusters a boxplot representation of $\log_2$ fold changes in expression between infected and mock-treated lungs is also shown for a more quantitative assessment of the changes in transcript levels.

A clearly defined small cluster (*cluster A*) composed of 18 of 378 genes (4.8%) includes transcripts whose relative expression levels were decreased with respect to their mock controls. Decreased expression after infection was less pronounced in the MyD88$^{-/-}$ group. A second group (*cluster B*) comprises 102 genes (27.2%) that were upregulated in WT and also in MyD88$^{-/-}$ mice after infection. On average, induction of these genes was stronger in WT mice, indicating that they depended partially on MyD88. In contrast, the third group (*cluster C*) contains 37 genes (9.5%) that were upregulated more strongly in response to the infection in MyD88$^{-/-}$ mice. The last and largest group (*cluster D*) consists of 221 genes (58.5%) that were upregulated in WT but not (or only weakly) in MyD88$^{-/-}$ mice. These MyD88-dependent genes are implicated mainly in immune responses. Representative genes for every cluster defined are listed in Table 1.

The observation that the majority of changes in the pulmonary transcriptome at *day 3* after infection are MyD88 dependent demonstrates the importance of this signaling pathway in the host response to *C. pneumoniae*. This difference at the transcriptome level is associated with decreased bacterial bur-

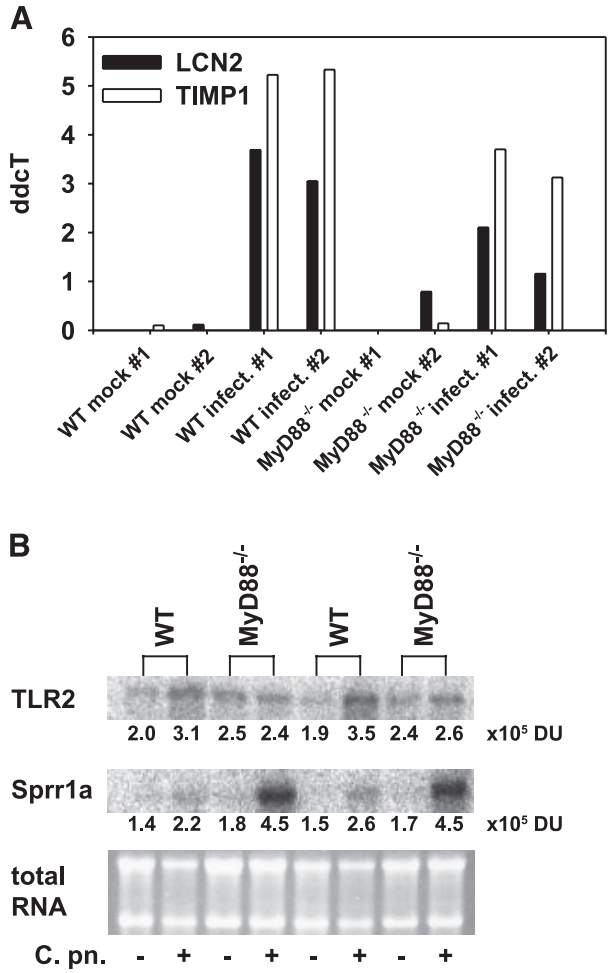

Fig. 3. Validation of MyD88-dependent and -independent mRNA expression. Total RNA was obtained from lungs of WT or MyD88$^{-/-}$ mice infected (infect.) with 2.5×10^6 inclusion-forming units (IFUs)/mouse *Chlamydia pneumoniae* (C.pn.), 3 days postinfection, or mock-infected mice as controls. TIMP1, tissue inhibitor of metalloproteinase-1; LCN2, lipocalin-2; TLR2, Toll-like receptor-2; C_T, threshold cycle; ddcT, $\Delta\Delta$CT. *A*: real-time RT-PCR was used to quantify *lcn2* and *timp1* as described in EXPERIMENTAL PROCEDURES. Data shown are mean values of PCR replicates from individual mice. *B*: expression of *tlr2* and *sprr1a* was analyzed by Northern blot, and the density of each band was quantified by ImageJ 1.37v (National Institutes of Health; **htpp://rsb.info.nih.gov/ij/**). Nos. are depicted at *bottom* and expressed as density units (DU). Ethidium bromide-stained ribosomal RNA bands are shown as loading controls.

Table 2. *Analysis of MeSH categories*

	Cluster A			*Cluster B*			*Cluster C*			*Cluster D*		
	Obs	Exp	z-Score	Obs	Exp	z-Score	Obs	Exp	z-Score	Obs	Exp	z-Score
Immune response												
Cytokines	46	119	−7	1,364	1,571	−6	80	250	−12	20,737	5,973	219
Chemokines	1	11	−3	96	143	−4	0	ND	ND	4,477	543	175
NF-kappa B	3	9	−2	205	119	8	32	19	3	3,873	453	166
Neutrophil infiltration	0	ND	ND	2	4	−1	0	ND	ND	81	16	17
Mycloid cells	8	37	−5	275	492	−10	26	78	−6	7,273	1,870	132
Cell cycle												
Cyclins	7	7	0	331	92	25	452	15	115	153	351	−11
Mitosis	0	0	0	63	39	4	227	6	89	36	147	−9
DNA damage	8	6	1	181	83	11	96	13	23	181	315	−8

Analysis of overrepresentation of medical subject heading (MeSH) terms for transcripts corresponding to *clusters A–D.* A high z-score indicates a significant overrepresentation of a category. ND, not determined; Obs, observed; Exp, expected.

den at this time point and lethal outcome later after infection (48, 49).

We have previously demonstrated that infected TLR2/TLR4 double-deficient mice showed a similar phenotype as MyD88$^{-/-}$ mice in terms of survival, chlamydial burden in lungs, and decreased granulocyte recruitment after 3 days of infection (48, 49). Therefore, we believe that differences in the transcriptome of WT vs. MyD88$^{-/-}$ mice were due to impaired TLR signaling in the latter mice. However, we cannot exclude the possibility that the nonfunctional IL-1 receptor signaling cascade in MyD88$^{-/-}$ mice was also in part responsible for the differences observed.

Expression of IFN-regulated genes is partially dependent on MyD88. Genes grouped within *cluster B* (Fig. 2) share the characteristic that their transcription in vivo depends only partially on MyD88 after 3 days of infection with *C. pneumoniae*. Strikingly, this group contains many genes whose transcription is induced by IFN (Table 1), although we were not able to detect IFN-γ or type I IFN in MyD88$^{-/-}$ mice, either by microarray or by ELISA at this point in time. In WT mice IFN-γ was increased 3 days postinfection (48), while type I IFN was again not detectable (data not shown). In accordance with our results, it was observed recently that IFN-γ secretion induced by *C. pneumoniae* in vitro depends on MyD88 (45, 50).

Whether the upregulation of IFN-induced genes in MyD88$^{-/-}$ mice is indeed caused by IFNs that escaped our attempts to detect them, or is rather due to other, to date unknown, factors capable of triggering the IFN-type response, remains to be elucidated (10). Of note, IFN-independent induction of IFN-stimulated gene (ISG) expression has been reported (11).

Other genes listed within *cluster B* belong to the family of cathepsins, like cathepsin K (*ctsk*), Z (*ctsz*), and S (*ctss*). These are proteolytic enzymes found in animal tissues that catalyze the hydrolysis of proteins into polypeptides (15) and are increased substantially in interstitial lung diseases (31). Cathepsin S is involved in regulation of antigen presentation and immunity (46) and is upregulated on IFN-γ stimulation (56), suggesting once more that this cytokine might have been secreted in MyD88$^{-/-}$ mice after infection with *C. pneumoniae*. Another gene from *cluster B* with a potential role in the control of chlamydial replication is lipocalin-2, whose partially MyD88-dependent induction was confirmed by real-time RT-PCR (Fig. 3*A*). Lipocalin-2 (*lcn2*) binds to bacterial enterochelins, thereby sequestering iron and depriving pathogens like *Escherichia coli* of this essential growth factor (17, 18). Furthermore, it has recently been published that, in macrophages stimulated with heat-killed group B streptococci (GBS), the induction of lipocalin-2 was severely impaired in the absence of TLR2 signaling (13). Thus the role of lipocalin in *C. pneumoniae* infection deserves further investigation.

Also, we could identify a set of genes whose function is related to membrane maintenance and cytoskeleton (Table 1). One member of this group is tenascin C, which is involved in tissue repair and is usually increased after an inflammatory process (41).

Tissue inhibitor of metalloproteinase-1 (*timp1*) was found as the most upregulated gene in MyD88$^{-/-}$ mice after infection with *C. pneumoniae*, and its presence was confirmed by real-time RT-PCR (Fig. 3*A*). This protein has been recently described to enhance pathology during infections. For instance, TIMP1-deficient mice are resistant to *Pseudomonas aeruginosa* corneal infection and show reduced lethality on pulmonary infection with the same microorganism (36). Therefore, the function of *timp1* may be important for the elucidation of

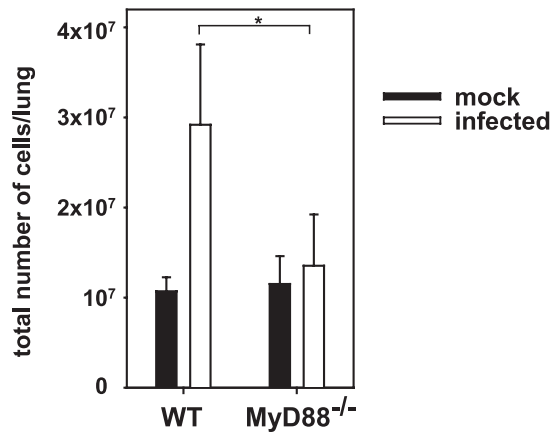

Fig. 4. Pulmonary inflammation 3 days postinfection with *C. pneumoniae*. The total cellular content from lungs of WT or MyD88$^{-/-}$ mice infected with 2.5×10^6 IFUs of *C. pneumoniae* ($n = 4$, black bars) was quantified. Mock-infected mice ($n = 2$, open bars) were used as control. Error bars represent SD. *$P = 0.028$, *t*-test.

the mechanisms involved in the lethal outcome of *C. pneumoniae* infection in MyD88$^{-/-}$ mice.

Genes involved in cell cycle control are upregulated more strongly in MyD88$^{-/-}$ mice. Cluster C depicted in Fig. 2 includes transcripts that were upregulated postinfection with *C. pneumoniae* in WT and MyD88$^{-/-}$ mice, i.e., are MyD88 independent. In fact, most of these genes were induced more strongly in the absence of MyD88. The cluster comprises a total of 37 genes, and, interestingly, all of them are connected to cell cycle control and DNA replication (Table 1). Furthermore, analysis with the Genomatix Bibliosphere software tool showed strong overrepresentation of the medical subject heading (MeSH) terms "cyclins," "mitosis," and "DNA damage" (Table 2). Northern blot analysis confirmed the MyD88-independent induction of transcription of the gene *sprr1a* (Fig. 3*B*).

It has been described already that MyD genes, e.g., *irf-1*, *jun*, *egr-1*, *myd116/gadd34*, and *myd118/gadd45b*, play a role in negative growth control including growth arrest and apoptosis (37, 38). MyD88 was originally characterized as a novel MyD gene in M1 myeloblastic leukemia cells induced for terminal macrophage differentiation by IL-6 (39), and ectopic expression of MyD88 in human cervical carcinoma HeLa cells was observed to induce apoptosis (27). Our data suggest that, aside from its crucial role as key adapter in the TLR signaling cascade, MyD88 may participate in the negative regulation of cellular growth. Alternatively, there may be an increased influx

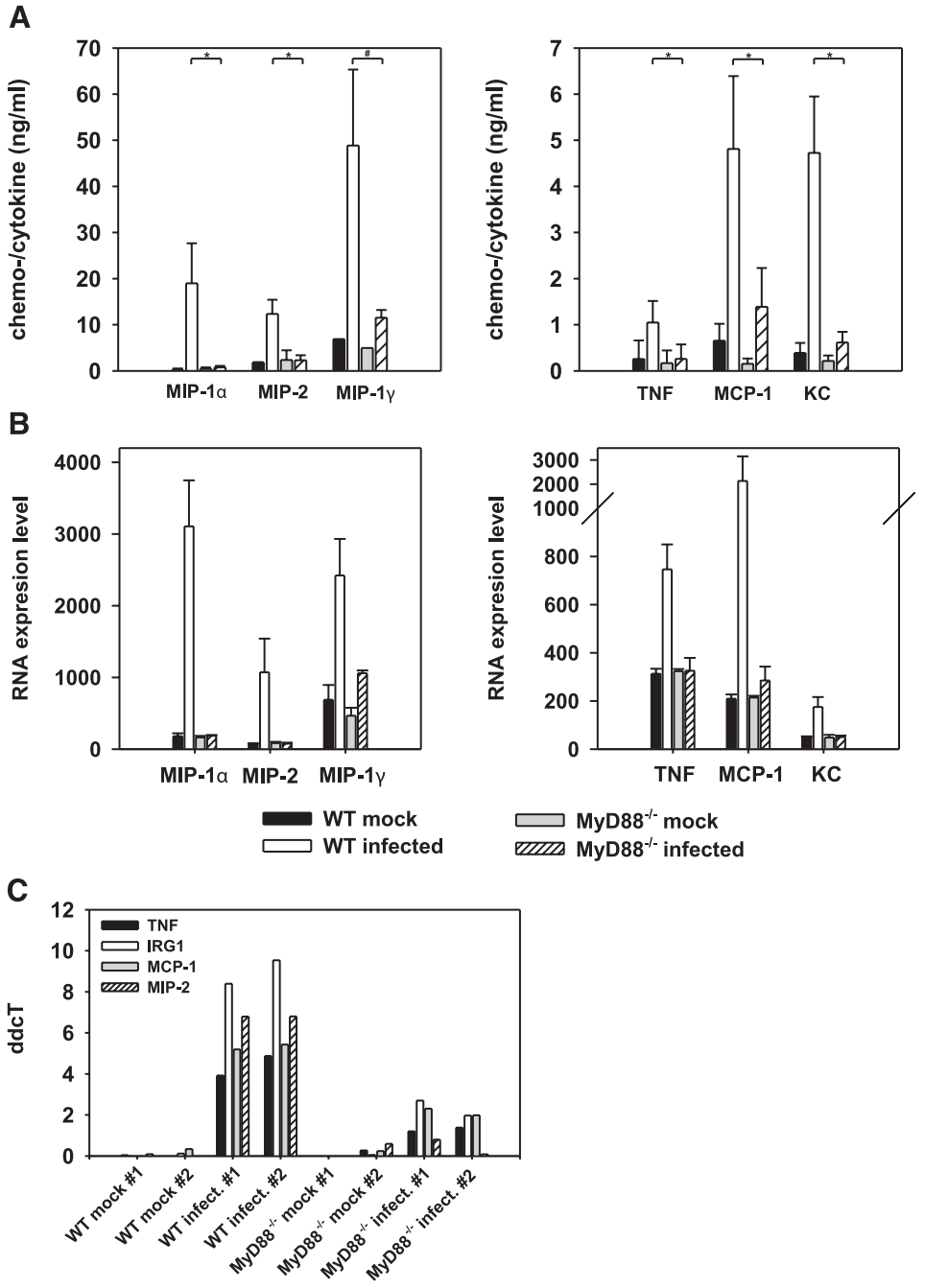

Fig. 5. Cytokine, chemokine, and *irg1* expression levels from lungs of WT and MyD88$^{-/-}$ mice after infection with *C. pneumoniae*. *A*: protein levels in supernatants of minced lungs. WT mice and MyD88$^{-/-}$ mice [$n = 9$, tumor necrosis factor (TNF) and keratinocyte-derived chemokine (KC); $n = 6$, macrophage inflammatory protein-1α (MIP-1α), MIP-2, and monocyte chemoattractant protein-1 (MCP-1); $n = 3$, MIP-1γ; open bars and hatched bars, respectively] were infected intranasally with 2.5×10^6 IFUs of *C. pneumoniae*. Mock-infected WT mice and MyD88$^{-/-}$ mice ($n = 3$, TNF and KC; $n = 2$, MIP-1α, MIP-2, and MCP-1; $n = 1$, MIP-1γ; black bars and gray bars, respectively) were used as controls. The levels of MIP-1α, MIP-2, TNF, MCP-1, KC, and MIP-1γ were determined by ELISA after 3 days of infection. Error bars represent the SD of equally treated mice. *$P \leq 0.002$, Mann-Whitney rank sum test; #$P = 0.01$, *t*-test. *B*: RNA expression level from cyto- and chemokines on the microarray chips. Averaged normalized absolute expression values of 3 biological replicates are shown. Error bars represent SD. *C*: real-time RT-PCR validation of microarray data for *irg1*, *tnf*, *mip-2*, and *mcp-1*. The PCR was performed as described in EXPERIMENTAL PROCEDURES.

of immature myeloid progenitors from the bone marrow that are still in the cell cycle in MyD88$^{-/-}$ mice. However, we consider this possibility as unlikely, since the pulmonary cellular content was not increased in MyD88$^{-/-}$ mice 3 days postinfection (Fig. 4).

MyD88-dependent genes are mainly involved in immune responses against C. pneumoniae infection. Cluster D contains 221 probe sets, corresponding to 208 unique genes with increased pulmonary expression on infection with *C. pneumoniae* in a MyD88-dependent fashion (Fig. 2). Approximately 70% of the genes within this cluster (149 genes) are annotated with the gene ontology term "immunological processes," indicating an overrepresentation of genes involved in immune responses. Strongest MyD88-dependent gene upregulation by *C. pneumoniae* infection was recorded for the immunoresponsive gene-1 (*irg1*), arginase-1 (*arg1*), and the cytokine TNF (*tnf*) or chemokines like MIP-1α (*ccl3*), MIP-2 (*cxcl2*), MCP-1 (*ccl2*), MIP-1γ (*ccl9*), and KC (*cxcl1*) (Table 1). To test whether the transcript levels determined by microarrays corresponded to protein levels, we analyzed the cyto- and chemokines secreted from supernatants of minced lungs of WT and MyD88$^{-/-}$ mice before and after the infection. Infected WT mice secreted MIP-1α, MIP-2, and KC in high amounts compared with the noninfected mice. However, MyD88$^{-/-}$ mice failed to secrete these chemokines on infection (Fig. 5*A*). TNF was secreted in a MyD88-dependent manner, and this upregulation was also confirmed by real-time RT-PCR (Fig. 5, *A* and *C*). In contrast, the chemokines MCP-1 and MIP-1γ were secreted by both groups of mice in response to the infection, although they were significantly reduced in MyD88$^{-/-}$ mice (Fig. 5*A*). These results were in accordance with the microarray RNA expression level (Fig. 5*B*). However, although the chemokine IP-10 (*cxcl10*) was the most upregulated in WT mice by microarray, we were not able to detect it by ELISA (data not shown).

Immunoresponsive gene-1 (*irg1*) was cloned from a cDNA library prepared with RNA isolated from macrophages after lipopolysaccharide (LPS) stimulation (35), and it belongs to the family of IFN-inducible genes (59). *Irg1* was found to be one of the most upregulated genes in WT mice after infection with *C. pneumoniae* (Table 1 and Fig. 5*C*) and also in the infected macrophage cell line ANA-1 in vitro (Table 3).

Further bioinformatic analysis with Genomatix Bibliosphere showed strong overrepresentation of the MeSH terms "neutrophil infiltration" and "myeloid cells" for *cluster D* (Table 2). Specifically, mRNA coding for the cell type-specific proteins neutrophil cytosolic factor-1 (*ncf1*), *ncf2* and *ncf4*, the receptor for granulocyte colony-stimulating factor (*csf3r*), and *mmp8* was upregulated in a MyD88-dependent manner. These findings are consistent with a recruitment of neutrophils and macrophages to the lungs of WT but not MyD88$^{-/-}$ mice, a difference we have indeed observed previously (48, 49). In addition, several factors with a role in attracting leukocytes are found in *cluster D*, including the chemokines *cxcl1* (KC) and *cxcl2* (MIP-2). Thus the cluster of MyD88-dependent genes identified here demonstrates the dependence of the inflammatory response on MyD88 and points to a lack of chemokine expression as explanation for the impaired influx of granulocytes in the absence of MyD88 signaling (Fig. 4). We are fully aware that the dynamic cellular composition of the lung in the course of infection and the use of whole lung RNA samples do not allow us to determine the relative contribution of transcriptional induction or repression in resident lung cells compared with the effect of leukocyte influx and migration. In an attempt to dissect this question by stopping leukocyte migration, we killed mice 3 h after infection and cultured the isolated lung pieces for an additional 24 h in vitro before measuring changes in gene expression. In this experiment, we found comparably little induction in infected lungs (data not shown). However, to answer this question in a technically satisfactory way, ventilation and perfusion of explanted and infected lungs would be required to allow direct comparison with the data presented here.

Finally, TLR2 is upregulated in response to *C. pneumoniae* infection in WT mice but much weaker in MyD88$^{-/-}$ mice (Fig. 3*B*). We have shown earlier that this microorganism is stimulating the immune response mainly via TLR2 (49). Whether upregulated expression of TLR2 and recognition of *C. pneumoniae* via TLR2 are connected remains to be shown.

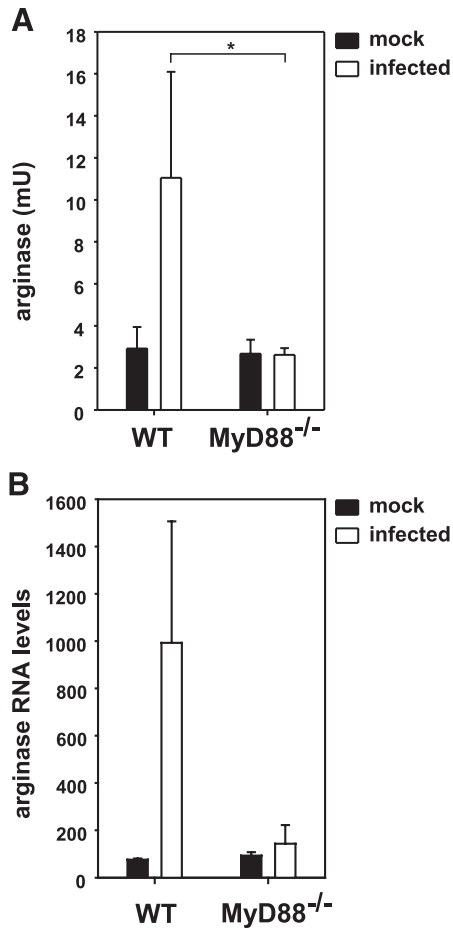

Fig. 6. *A*: arginase activity in lung homogenates after *C. pneumoniae* infection. WT or MyD88$^{-/-}$ mice were mock infected ($n = 3$, black bars) or infected with *C. pneumoniae* ($n = 5$ for WT and $n = 6$ for MyD88$^{-/-}$, open bars). After 3 days, lungs were removed, and arginase activity was measured. Error bars represent SD. *$P = 0.004$, Mann-Whitney rank sum test. *B*: RNA expression level of arginase-1 determined by microarrays. Averaged normalized absolute expression values of 3 individual mice are shown. Error bars represent the SD.

Table 3. *Gene induction in ANA-1 macrophages compared with the in vivo data*

Probe Set	Gene Title	Gene Symbol	ANA-1 FC	Lung WT FC	Lung MyD88$^{-/-}$ FC
1450826_a_at	serum amyloid A 3	Saa3	17.4	16.7	2.6
1449984_at	chemokine (C-X-C motif) ligand 2	Cxcl2	12.8	14.5	0.9
1427381_at	immunoresponsive gene 1	Irg1	9.1	20.1	1.1
1417262_at	prostaglandin-endoperoxide synthase 2	Ptgs2	7.8	1.7	1.1*
1421228_at	chemokine (C-C motif) ligand 7	Ccl7	6.5	5.4	1.4
1419561_at	chemokine (C-C motif) ligand 3	Ccl3	5.3	17.2	1.1
1417483_at	molecule possessing ankyrin-repeats induced by lipopolysaccharide	Mail-pending	4.8	2.4	1.2
1419607_at	tumor necrosis factor	Tnf	4.5	2.4	1.0
1421578_at	chemokine (C-C motif) ligand 4	Ccl4	4.2	6.3	0.9
1423233_at	CCAAT/enhancer binding protein (C/EBP), delta	Cebpd	3.8	1.1	1.0*
1422619_at	phosphatidic acid phosphatase 2a	Ppap2a	3.5	0.7	0.8*
1427725_a_at	POU domain, class 2, transcription factor 2	Pou2f2	3.1	1.2	1.1*
1449399_a_at	interleukin 1 beta	Illb	2.8	5.6	1.2
1448610_a_at	superoxide dismutase 2, mitochondrial	Sod2	2.6	2.7	1.4
1426441_at	solute carrier family 11, member 2	Slc11a2	2.5	1.2	0.9*
1417813_at	inhibitor of kappaB kinase epsilon	Ikbke	2.5	3.5	1.2
1420394_s_at	glycoprotein 49 B	Gp49b	2.5	4.8	2.5
1422978_at	cytochrome b-245, beta polypeptide	Cybb	2.5	2.4	1.4
1419004_s_at	B-cell leukemia/lymphoma 2 related protein A1a hypothetical protein	Bcl2a1a	2.4	3.6	1.9
1437111_at	A230108E06	A230108E06	2.4	1.0	0.9*
1418099_at	tumor necrosis factor receptor superfamily, member 1b	Tnfrsf1b	2.4	3.1	1.4
1449498_at	macrophage receptor with collagenous structure	Marco	2.3	4.2	2.5

Expression values of the 22 significantly regulated genes in ANA-1 macrophages infected with *C. pneumoniae* juxtaposed to the in vivo data. Values for the ANA-1 set represent the average of 2 experiments. FC, fold change. *Genes induced in ANA-1 cells but not in vivo in WT and MyD88$^{-/-}$ mice.

Pulmonary infection with C. pneumoniae leads to an increase in arginase activity in a MyD88-dependent manner. Another highly upregulated gene observed by microarray analysis is arginase-1 (*arg1*), which is included within the MyD88-dependent cluster. This finding was confirmed by a functional assay and increased activity of arginase was present in lungs of WT mice in response to the infection with *C. pneumoniae* (Fig. 6*A*). In contrast, infected MyD88$^{-/-}$ mice showed similar levels of arginase enzymatic activity as the mock control. These results correlate with the pattern of *arg1* mRNA levels observed in the microarray (Fig. 6*B*). Average expression levels of arginase 2 were increased twofold in infected WT but not in MyD88$^{-/-}$ lungs without reaching statistical significance (data not shown). Therefore, although arginase 2 can contribute to the enzymatic activity as shown in Fig. 6*A*, the bulk of induced arginase activity is likely caused by arginase-1.

Arginase-1 is constitutively expressed in hepatocytes where it is the key enzyme of the urea cycle. In addition, high level expression of arginase-1 is inducible in macrophages by the Th2 cytokines IL-4, IL-13, and IL-10 (43). Whether macrophages express in vivo arginase-1 on pulmonary infection with *C. pneumoniae* remains to be shown. Arginase-1 hydrolyzes arginine to urea and L-ornithine, which is the precursor for the production of polyamines, which are essential for cell proliferation (42). A role for arginase-1 in promotion of tissue fibrosis has been suggested in schistosomiasis. In this model, Th2 cytokines induce arginase-1 to produce L-ornithine, which is metabolized to proline by the enzyme ornithine aminotransferase (24). Either an increase in arginase induced by a Th2 response or upregulated synthesis of proline may explain increased collagen deposition in this model of schistosomiasis (51, 55). Future studies could investigate whether similar mechanisms take place during infection with *C. pneumoniae*.

Correlation of gene induction between C. pneumoniae-infected lungs and the in vitro infected macrophage cell line ANA-1. In parallel, we have also analyzed the gene expression pattern of mouse macrophages (ANA-1 cells) after the infection in vitro with *C. pneumoniae*. Twenty-two genes were significantly upregulated (Table 3). From these, 16 genes (72.7%) were also induced in the lungs of infected mice, and all of them were grouped within the cluster of MyD88-dependent genes with the exception of glycoprotein-49B (*gp49b*) and macrophage receptor with collagenous structure (*marco*), which were found to be partially MyD88 dependent. Examples of the most upregulated genes in mouse macrophages after *C. pneumoniae* infection are serum amyloid A3 (*saa3*), a protein that is mainly produced by activated macrophages during tissue injury or inflammation, MIP-2 (*cxcl2*), and *irg1*. Expression levels of all genes induced by *C. pneumoniae* in macrophages in vitro correlated with the results obtained from infected lungs from WT mice, suggesting that this cell type participates in host defense in vivo against *C. pneumoniae*.

The fact that *C. pneumoniae*-induced transcriptional changes in ANA-1 macrophages are relatively weak compared with the hundreds of significantly regulated genes in the lung after infection in vivo highlights the advantage of the experimental approach we used. Since many questions regarding the biology of respiratory chlamydial infection are unclear at present, the alternative approach of analyzing the transcriptome of selected purified cell types, e.g., alveolar macrophages or lung epithelial cells, most likely would have missed an essential part of the picture. Given the complexity of the in vivo response to infection, it will now be important to dissect the contribution of different cell types to the transcriptional responses discussed above. This study and recently reported studies (12, 28, 30) show that profiling of lung tissue RNA can be used to identify patterns of gene expression during infection and inflammation dependent on host factors, pathogen strain, or timing.

ACKNOWLEDGMENTS

The excellent technical assistance of Angela Servatius is appreciated. We thank Katrin Mair for primers for lipocalin-2 RT-PCR, Susi Dürr for *C. pneumoniae* purification, and Jila Navai for excellent technical assistance. We are grateful to Dr. Ines Corraliza for helping to analyze the activity of arginase.

GRANTS

This work was funded in part by the Bundesministerium für Bildung und Forschung (NGFN-2 Grant No. 01GS0402 TP37) to R. Lang, H. Wagner, and R. Hoffmann.

REFERENCES

1. **Araki A, Kanai T, Ishikura T, Makita S, Uraushihara K, Iiyama R, Totsuka T, Takeda K, Akira S, Watanabe M.** MyD88-deficient mice develop severe intestinal inflammation in dextran sodium sulfate colitis. *J Gastroenterol* 40: 16–23, 2005.
2. **Belland RJ, Ouellette SP, Gieffers J, Byrne GI.** Chlamydia pneumoniae and atherosclerosis. *Cell Microbiol* 6: 117–127, 2004.
3. **Blasi F, Tarsia P, Arosio C, Fagetti L, Allegra L.** Epidemiology of *Chlamydia pneumoniae*. *Clin Microbiol Infect* 4, *Suppl* 4: S1–S6, 1998.
4. **Bolstad BM, Irizarry RA, Astrand M, Speed TP.** A comparison of normalization methods for high density oligonucleotide array data based on variance and bias. *Bioinformatics* 19: 185–193, 2003.
5. **Campos MA, Closel M, Valente EP, Cardoso JE, Akira S, Alvarez-Leite JI, Ropert C, Gazzinelli RT.** Impaired production of proinflammatory cytokines and host resistance to acute infection with *Trypanosoma cruzi* in mice lacking functional myeloid differentiation factor 88. *J Immunol* 172: 1711–1718, 2004.
6. **Chuang T, Ulevitch RJ.** Identification of hTLR10: a novel human Toll-like receptor preferentially expressed in immune cells. *Biochim Biophys Acta* 1518: 157–161, 2001.
7. **Clementsen P, Permin H, Norn S.** *Chlamydia pneumoniae* infection and its role in asthma and chronic obstructive pulmonary disease. *J Investig Allergol Clin Immunol* 12: 73–79, 2002.
8. **Corraliza IM, Campo ML, Soler G, Modolell M.** Determination of arginase activity in macrophages: a micromethod. *J Immunol Methods* 174: 231–235, 1994.
9. **Cunningham AF, Johnston SL, Julious SA, Lampe FC, Ward ME.** Chronic *Chlamydia pneumoniae* infection and asthma exacerbations in children. *Eur Respir J* 11: 345–349, 1998.
10. **Decker T, Muller M, Stockinger S.** The yin and yang of type I interferon activity in bacterial infection. *Nat Rev Immunol* 5: 675–687, 2005.
11. **DeFilippis V, Fruh K.** Rhesus cytomegalovirus particles prevent activation of interferon regulatory factor 3. *J Virol* 79: 6419–6431, 2005.
12. **Domachowske JB, Bonville CA, Easton AJ, Rosenberg HF.** Differential expression of proinflammatory cytokine genes in vivo in response to pathogenic and nonpathogenic pneumovirus infections. *J Infect Dis* 186: 8–14, 2002.
13. **Draper DW, Bethea HN, He YW.** Toll-like receptor 2-dependent and -independent activation of macrophages by group B streptococci. *Immunol Lett* 102: 202–214, 2006.
14. **Du X, Poltorak A, Wei Y, Beutler B.** Three novel mammalian toll-like receptors: gene structure, expression, and evolution. *Eur Cytokine Netw* 11: 362–371, 2000.
15. **Fajardo I, Svensson L, Bucht A, Pejler G.** Increased levels of hypoxia-sensitive proteins in allergic airway inflammation. *Am J Respir Crit Care Med* 170: 477–484, 2004.
16. **Ferrari M, Poli A, Olivieri M, Verlato G, Tardivo S, Nicolis M, Campello C.** Respiratory symptoms, asthma, atopy and Chlamydia pneumoniae IgG antibodies in a general population sample of young adults. *Infection* 30: 203–207, 2002.
17. **Fischbach MA, Lin H, Zhou L, Yu Y, Abergel RJ, Liu DR, Raymond KN, Wanner BL, Strong RK, Walsh CT, Aderem A, Smith KD.** The pathogen-associated iroA gene cluster mediates bacterial evasion of lipocalin 2. *Proc Natl Acad Sci USA* 103: 16502–16507, 2006.
18. **Flo TH, Smith KD, Sato S, Rodriguez DJ, Holmes MA, Strong RK, Akira S, Aderem A.** Lipocalin 2 mediates an innate immune response to bacterial infection by sequestrating iron. *Nature* 432: 917–921, 2004.
19. **Fremond CM, Yeremeev V, Nicolle DM, Jacobs M, Quesniaux VF, Ryffel B.** Fatal *Mycobacterium tuberculosis* infection despite adaptive immune response in the absence of MyD88. *J Clin Invest* 114: 1790–1799, 2004.
20. **Gaydos CA, Summersgill JT, Sahney NN, Ramirez JA, Quinn TC.** Replication of *Chlamydia pneumoniae* in vitro in human macrophages, endothelial cells, and aortic artery smooth muscle cells. *Infect Immun* 64: 1614–1620, 1996.
21. **Grayston JT.** Background and current knowledge of *Chlamydia pneumoniae* and atherosclerosis. *J Infect Dis* 181, *Suppl* 3: S402–S410, 2000.
22. **Grayston JT.** *Chlamydia pneumoniae* and atherosclerosis. *Clin Infect Dis* 40: 1131–1132, 2005.
23. **Hemmi H, Takeuchi O, Kawai T, Kaisho T, Sato S, Sanjo H, Matsumoto M, Hoshino K, Wagner H, Takeda K, Akira S.** A Toll-like receptor recognizes bacterial DNA. *Nature* 408: 740–745, 2000.
24. **Hesse M, Modolell M, La Flamme AC, Schito M, Fuentes JM, Cheever AW, Pearce EJ, Wynn TA.** Differential regulation of nitric oxide synthase-2 and arginase-1 by type 1/type 2 cytokines in vivo: granulomatous pathology is shaped by the pattern of L-arginine metabolism. *J Immunol* 167: 6533–6544, 2001.
25. **Jahn HU, Krull M, Wuppermann FN, Klucken AC, Rosseau S, Seybold J, Hegemann JH, Jantos CA, Suttorp N.** Infection and activation of airway epithelial cells by *Chlamydia pneumoniae*. *J Infect Dis* 182: 1678–1687, 2000.
26. **Jaremo P, Richter A.** *Chlamydia pneumoniae* IgG and the severity of coronary atherosclerosis. *Eur J Intern Med* 15: 508–510, 2004.
27. **Jaunin F, Burns K, Tschopp J, Martin TE, Fakan S.** Ultrastructural distribution of the death-domain-containing MyD88 protein in HeLa cells. *Exp Cell Res* 243: 67–75, 1998.
28. **Jeyaseelan S, Chu HW, Young SK, Worthen GS.** Transcriptional profiling of lipopolysaccharide-induced acute lung injury. *Infect Immun* 72: 7247–7256, 2004.
29. **Johnston SL.** Influence of viral and bacterial respiratory infections on exacerbations and symptom severity in childhood asthma. *Pediatr Pulmonol Suppl* 16: 88–89, 1997.
30. **Kash JC, Basler CF, Garcia-Sastre A, Carter V, Billharz R, Swayne DE, Przygodzki RM, Taubenberger JK, Katze MG, Tumpey TM.** Global host immune response: pathogenesis and transcriptional profiling of type A influenza viruses expressing the hemagglutinin and neuraminidase genes from the 1918 pandemic virus. *J Virol* 78: 9499–9511, 2004.
31. **Kimura M, Tani K, Miyata J, Sato K, Hayashi A, Otsuka S, Urata T, Sone S.** The significance of cathepsins, thrombin and aminopeptidase in diffuse interstitial lung diseases. *J Med Invest* 52: 93–100, 2005.
32. **Koedel U, Rupprecht T, Angele B, Heesemann J, Wagner H, Pfister HW, Kirschning CJ.** MyD88 is required for mounting a robust host immune response to *Streptococcus pneumoniae* in the CNS. *Brain* 127: 1437–1445, 2004.
33. **Kuo CC, Jackson LA, Campbell LA, Grayston JT.** *Chlamydia pneumoniae* (TWAR). *Clin Microbiol Rev* 8: 451–461, 1995.
34. **Kwon TW, Kim do K, Ye JS, Lee WJ, Moon MS, Joo CH, Lee H, Kim YK.** Detection of enterovirus, cytomegalovirus, and Chlamydia pneumoniae in atheromas. *J Microbiol* 42: 299–304, 2004.
35. **Lee CG, Jenkins NA, Gilbert DJ, Copeland NG, O'Brien WE.** Cloning and analysis of gene regulation of a novel LPS-inducible cDNA. *Immunogenetics* 41: 263–270, 1995.
36. **Lee MM, Yoon BJ, Osiewicz K, Preston M, Bundy B, van Heeckeren AM, Werb Z, Soloway PD.** Tissue inhibitor of metalloproteinase 1 regulates resistance to infection. *Infect Immun* 73: 661–665, 2005.
37. **Liebermann DA, Hoffman B.** MyD genes in negative growth control. *Oncogene* 17: 3319–3329, 1998.
38. **Liebermann DA, Hoffman B.** Myeloid differentiation (MyD) primary response genes in hematopoiesis. *Blood Cells Mol Dis* 31: 213–228, 2003.
39. **Lord KA, Hoffman-Liebermann B, Liebermann DA.** Nucleotide sequence and expression of a cDNA encoding MyD88, a novel myeloid differentiation primary response gene induced by IL6. *Oncogene* 5: 1095–1097, 1990.
40. **Maass M, Harig U.** Evaluation of culture conditions used for isolation of *Chlamydia pneumoniae*. *Am J Clin Pathol* 103: 141–148, 1995.
41. **Midwood KS, Valenick LV, Hsia HC, Schwarzbauer JE.** Coregulation of fibronectin signaling and matrix contraction by tenascin-C and syndecan-4. *Mol Biol Cell* 15: 5670–5677, 2004.
42. **Morris SM Jr.** Regulation of enzymes of the urea cycle and arginine metabolism. *Annu Rev Nutr* 22: 87–105, 2002.
43. **Munder M, Eichmann K, Moran JM, Centeno F, Soler G, Modolell M.** Th1/Th2-regulated expression of arginase isoforms in murine macrophages and dendritic cells. *J Immunol* 163: 3771–3777, 1999.
44. **Muzio M, Bosisio D, Polentarutti N, D'Amico G, Stoppacciaro A, Mancinelli R, van't Veer C, Penton-Rol G, Ruco LP, Allavena P,**

Mantovani A. Differential expression and regulation of toll-like receptors (TLR) in human leukocytes: selective expression of TLR3 in dendritic cells. *J Immunol* 164: 5998–6004, 2000.
45. **Netea MG, Kullberg BJ, Jacobs LE, Verver-Jansen TJ, van der Ven-Jongekrijg J, Galama JM, Stalenhoef AF, Dinarello CA, Van der Meer JW.** *Chlamydia pneumoniae* stimulates IFN-gamma synthesis through MyD88-dependent, TLR2- and TLR4-independent induction of IL-18 release. *J Immunol* 173: 1477–1482, 2004.
46. **Riese RJ, Mitchell RN, Villadangos JA, Shi GP, Palmer JT, Karp ER, De Sanctis GT, Ploegh HL, Chapman HA.** Cathepsin S activity regulates antigen presentation and immunity. *J Clin Invest* 101: 2351–2363, 1998.
47. **Rock FL, Hardiman G, Timans JC, Kastelein RA, Bazan JF.** A family of human receptors structurally related to Drosophila Toll. *Proc Natl Acad Sci USA* 95: 588–593, 1998.
48. **Rodriguez N, Fend F, Jennen L, Schiemann M, Wantia N, da Costa CU, Durr S, Heinzmann U, Wagner H, Miethke T.** Polymorphonuclear neutrophils improve replication of *Chlamydia pneumoniae* in vivo upon MyD88-dependent attraction. *J Immunol* 174: 4836–4844, 2005.
49. **Rodriguez N, Wantia N, Fend F, Durr S, Wagner H, Miethke T.** Differential involvement of TLR2 and TLR4 in host survival during pulmonary infection with *Chlamydia pneumoniae*. *Eur J Immunol* 36: 1145–1155, 2006.
50. **Rothfuchs AG, Trumstedt C, Wigzell H, Rottenberg ME.** Intracellular bacterial infection-induced IFN-gamma is critically but not solely dependent on Toll-like receptor 4-myeloid differentiation factor 88-IFN-alpha beta-STAT1 signaling. *J Immunol* 172: 6345–6353, 2004.
51. **Sandler NG, Mentink-Kane MM, Cheever AW, Wynn TA.** Global gene expression profiles during acute pathogen-induced pulmonary inflammation reveal divergent roles for Th1 and Th2 responses in tissue repair. *J Immunol* 171: 3655–3667, 2003.
52. **Scanga CA, Bafica A, Feng CG, Cheever AW, Hieny S, Sher A.** MyD88-deficient mice display a profound loss in resistance to *Mycobacterium tuberculosis* associated with partially impaired Th1 cytokine and nitric oxide synthase 2 expression. *Infect Immun* 72: 2400–2404, 2004.
53. **Schmidt SM, Muller CE, Bruns R, Wiersbitzky SK.** Bronchial *Chlamydia pneumoniae* infection, markers of allergic inflammation and lung function in children. *Pediatr Allergy Immunol* 12: 257–265, 2001.
54. **Shemer-Avni Y, Lieberman D.** Chlamydia pneumoniae-induced ciliostasis in ciliated bronchial epithelial cells. *J Infect Dis* 171: 1274–1278, 1995.
55. **Shi HP, Fishel RS, Efron DT, Williams JZ, Fishel MH, Barbul A.** Effect of supplemental ornithine on wound healing. *J Surg Res* 106: 299–302, 2002.
56. **Storm van's Gravesande K, Layne MD, Ye Q, Le L, Baron RM, Perrella MA, Santambrogio L, Silverman ES, Riese RJ.** IFN regulatory factor-1 regulates IFN-gamma-dependent cathepsin S expression. *J Immunol* 168: 4488–4494, 2002.
57. **Sturn A, Quackenbush J, Trajanoski Z.** Genesis: cluster analysis of microarray data. *Bioinformatics* 18: 207–208, 2002.
58. **Sugawara I, Yamada H, Mizuno S, Takeda K, Akira S.** Mycobacterial infection in MyD88-deficient mice. *Microbiol Immunol* 47: 841–847, 2003.
59. **Sugiyama T, Fujita M, Koide N, Mori I, Yoshida T, Mori H, Yokochi T.** 2-Aminopurine inhibits lipopolysaccharide-induced nitric oxide production by preventing IFN-beta production. *Microbiol Immunol* 48: 957–963, 2004.
60. **Takeda K, Akira S.** Toll-like receptors in innate immunity. *Int Immunol* 17: 1–14, 2005.
61. **Takeda K, Kaisho T, Akira S.** Toll-like receptors. *Annu Rev Immunol* 21: 335–376, 2003.
62. **Takeuchi O, Kawai T, Sanjo H, Copeland NG, Gilbert DJ, Jenkins NA, Takeda K, Akira S.** TLR6: a novel member of an expanding toll-like receptor family. *Gene* 231: 59–65, 1999.
63. **Tusher VG, Tibshirani R, Chu G.** Significance analysis of microarrays applied to the ionizing radiation response. *Proc Natl Acad Sci USA* 98: 5116–5121, 2001.
64. **van Zandbergen G, Gieffers J, Kothe H, Rupp J, Bollinger A, Aga E, Klinger M, Brade H, Dalhoff K, Maass M, Solbach W, Laskay T.** *Chlamydia pneumoniae* multiply in neutrophil granulocytes and delay their spontaneous apoptosis. *J Immunol* 172: 1768–1776, 2004.
65. **Weighardt H, Kaiser-Moore S, Vabulas RM, Kirschning CJ, Wagner H, Holzmann B.** Cutting edge: myeloid differentiation factor 88 deficiency improves resistance against sepsis caused by polymicrobial infection. *J Immunol* 169: 2823–2827, 2002.
66. **Yang J, Hooper WC, Phillips DJ, Tondella ML, Talkington DF.** Induction of proinflammatory cytokines in human lung epithelial cells during *Chlamydia pneumoniae* infection. *Infect Immun* 71: 614–620, 2003.
67. **Yang ZP, Cummings PK, Patton DL, Kuo CC.** Ultrastructural lung pathology of experimental *Chlamydia pneumoniae* pneumonitis in mice. *J Infect Dis* 170: 464–467, 1994.
68. **Yang ZP, Kuo CC, Grayston JT.** A mouse model of *Chlamydia pneumoniae* strain TWAR pneumonitis. *Infect Immun* 61: 2037–2040, 1993.
69. **Zhang D, Zhang G, Hayden MS, Greenblatt MB, Bussey C, Flavell RA, Ghosh S.** A toll-like receptor that prevents infection by uropathogenic bacteria. *Science* 303: 1522–1526, 2004.
70. **Zhou S, Kurt-Jones EA, Mandell L, Cerny A, Chan M, Golenbock DT, Finberg RW.** MyD88 is critical for the development of innate and adaptive immunity during acute lymphocytic choriomeningitis virus infection. *Eur J Immunol* 35: 822–830, 2005.